Supplement of Atmos. Chem. Phys., 20, 1277–1300, 2020
https://doi.org/10.5194/acp-20-1277-2020-supplement

Supplement of

Variability of hydroxyl radical (OH) reactivity in the Landes maritime pine forest: results from the LANDEX campaign 2017

Sandy Bsaibes et al.

Correspondence to: Sandy Bsaibes (sandy.bsaibes@gmail.com) and Valérie Gros (valerie.gros@lsce.ipsl.fr)

Supplement of:

Variability of OH reactivity in the Landes maritime Pine forest: Results from the LANDEX campaign 2017

Supplementary material 1: Data availability

Table S1. Timetable of the data available from each instrument measuring inside and / or above the canopy.

		June 2017								**July 2017**																		
		23	**24**	**25**	**26**	**27**	**28**	**29**	**30**	**1**	**2**	**3**	**4**	**5**	**6**	**7**	**8**	**9**	**10**	**11**	**12**	**13**	**14**	**15**	**16**	**17**	**18**	**19**
Above canopy (12 m)	**GC-NMHC**	🟪	🟪	🟪	🟪	🟪	🟪	🟪	🟪	🟪	🟪	🟪	🟪	🟪	🟪	🟪	🟪	🟪	🟪	🟪	🟪	🟪	🟪	🟪	🟪	🟪	🟪	🟪
	GC-OVOC			🟥	🟥	🟥	🟥	🟥	🟥	🟥	🟥	🟥	🟥	🟥	🟥	🟥	🟥	🟥	🟥	🟥	🟥	🟥	🟥	🟥	🟥			
	GC-BVOC1 LSCE							🟧	🟧	🟧	🟧	🟧	🟧	🟧	🟧	🟧	🟧	🟧	🟧	🟧	🟧	🟧	🟧	🟧	🟧	🟧	🟧	
	PTRQiToF-MS			🟦	🟦	🟦	🟦	🟦	🟦	🟦	🟦	🟦	🟦	🟦	🟦	🟦	🟦	🟦	🟦	🟦	🟦	🟦	🟦	🟦	🟦	🟦	🟦	🟦
Inside canopy (6 m)	**GC-BVOC2 IMT**							🟨	🟨	🟨	🟨	🟨	🟨	🟨	🟨	🟨	🟨	🟨	🟨	🟨	🟨	🟨						
	PTR-QiToFMS			🟦	🟦	🟦	🟦	🟦	🟦	🟦	🟦	🟦	🟦	🟦	🟦	🟦	🟦	🟦	🟦	🟦	🟦	🟦	🟦	🟦	🟦	🟦	🟦	🟦

Supplementary material 2: Consistency between GC-BVOC instruments and the PTR-MS on monoterpenes measurements

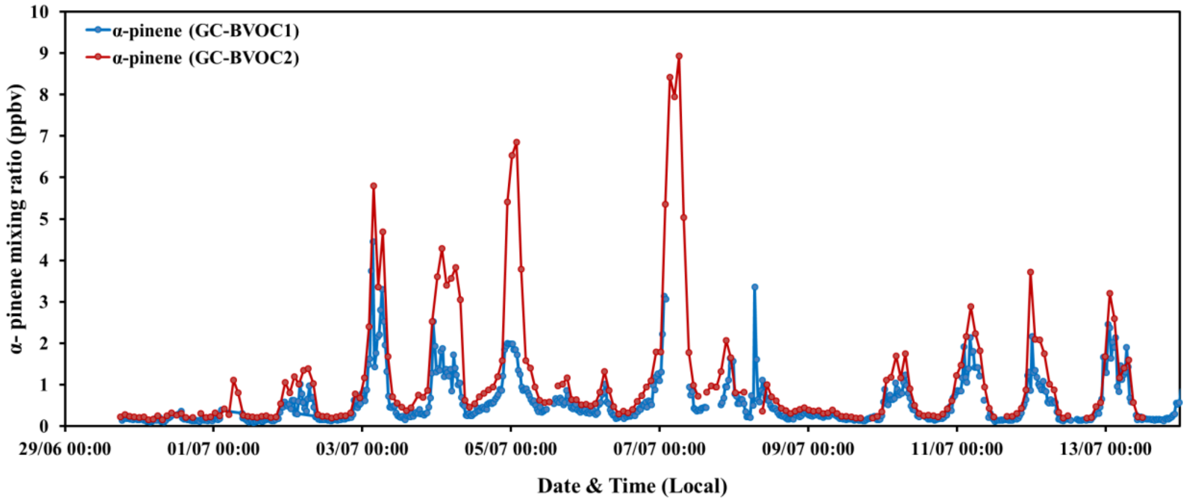

Figure S2(a). Variability of α-pinene mixing ratios measured at 12 m by the GC-BVOC1 (blue) and at 6 m by the GC BVOC2 (red).

Before the 13th of July, the consistency between the two GC-BVOC instruments was checked, taking into account the intercomparison of the standard cylinders used to calibrate each GC-BVOC. In addition, the profiles of the 8 species commonly measured by both GCs, were compared. Figure S2(a), shows the variability of α-pinene mixing ratios recorded by the GC-BVOC1 at 12 m height (blue) and by the GC-BVOC2 at 6 m height (red). The diurnal variability was demonstrated at both heights. Both instruments measured similar values during day-time when the vertical turbulence was higher and the mixing was more efficient within the canopy. However, a difference in the values recorded by the two GCs was seen during most nights, mainly related to the lower turbulence and the higher vertical stratification.

In order to verify the consistency between the GC instruments and the PTR-MS inside and above the canopy, the sum of the different monoterpenes concentrations measured by both GC-BVOCs and the sum of monoterpenes measured at *m/z* 137 + *m/z* 81 by the PTR-MS were compared.

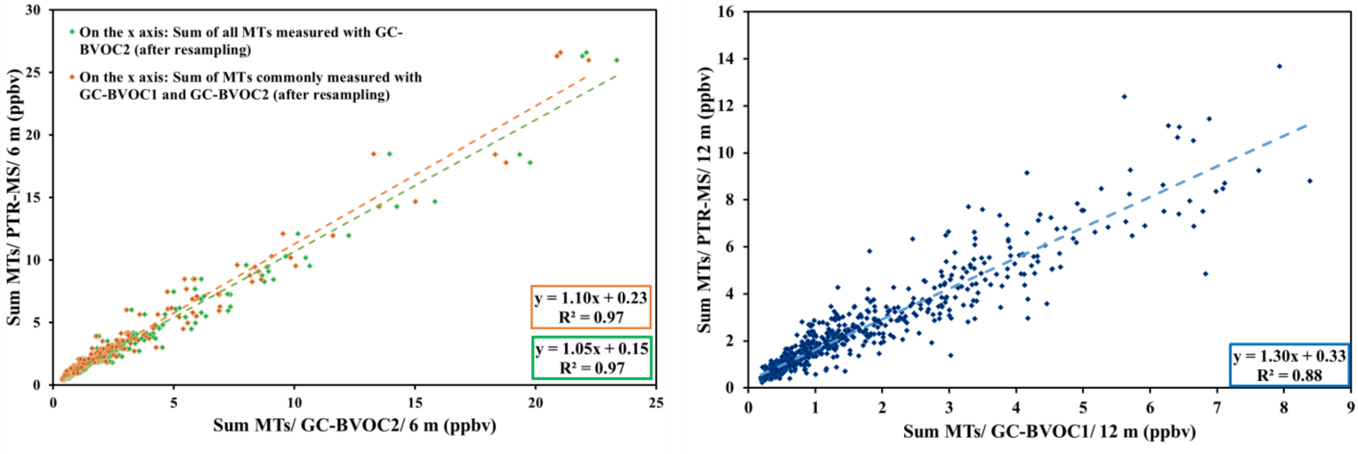

Figure S2. Correlation between (b) the sum of monoterpenes measured by the GC-BVOC2 and the PTR-MS at 6 m height and (c) the sum of monoterpenes measured by GC-BVOC1 and the PTR-MS at 12 m height. In Fig. S2b, green dots consider the sum of all BVOCs measured by the GC-BVOC2 whereas orange dots consider the sum of the monoterpenes measured by GC-BVOC2 which are commonly measured by the GC-BVOC1.

Figures S2b and c show that the concentrations are in good agreement most of the time. Higher concentrations were observed with the PTR-MS with a slope of 1.3 at 12 m. It is worth noting that a resampling of GC-BVOCs and PTR-MS datasets was made to get the same time base. As the GC-BVOC2 (6 m) has a time resolution of 90 min, the GC-BVOC1 (12 m) of 30 min and the PTR-MS of 30 min, a resampling using averaging with a time resolution of 90 min of the PTR-MS data and a linear interpolation was chosen for the comparison at 6 m height and a linear interpolation with a time resolution of 30 min at 12 m height.

The maximum difference between the sum of monoterpenes measured by the PTR-MS and all of the monoterpenes measured by the GC-BVOC2 at 6 m was 3.2 ppbv, whereas, the maximum difference between the sum of monoterpenes measured by the PTR-MS and the monoterpenes measured by the GC-BVOC2 which are commonly measured by GC-BVOC1 was 4.4 ppbv.

Supplementary material 3: Use of monoterpenes ratios in the weighted k rate coefficient calculation

Ratios of the different monoterpenes were calculated using GC-BVOC data at both heights. Figure S3a shows the ratios at 12 m height.

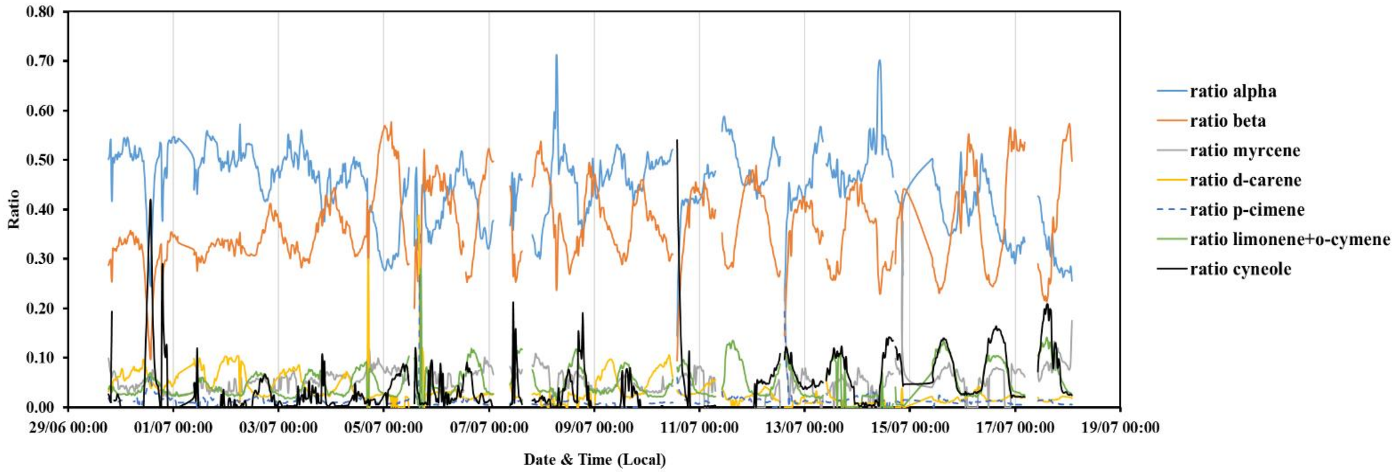

Figure S3(a). Ratio of all 8 monoterpenes calculated with the GC-BVOC1 data at 12 m height

Above canopy (12 m)

The comparison of the calculated OH reactivity from each monoterpene with the one obtained from the ratios for the GC-BVOC1 data and the PTR-MS data, regarding the overlapping period, is shown in Fig. S3b for the measurements at 12 m height. The use of the ratios in OH reactivity calculations is in good agreement with the use of individual monoterpenes and their respective k rate constants, except for some overestimations at the peaks, observed when using the PTR-MS data. It is worth noting that, cis-o-cimene is co-eluted with limonene. Therefore, the ratio of cis-o-cimene and limonene over their sum was calculated using the GC-BVOC2 data (average: 0.15/0.85 respectively).

When plotting the calculated OH reactivity from the sum of GC-BVOC1 monoterpenes and $k_{weighted}$ with the calculated OH reactivity using each individual monoterpene and its respective k rate constant, a slope of 0.96 was obtained, reflecting a good agreement (Fig. S3c). Whereas, a higher slope of 1.30 was obtained when considering the sum of monoterpenes from the PTR-QiToFMS data with $k_{weighted}$ (Fig. S3d). This observation is in agreement with the one made in figure S2c, when comparing the sum of monoterpenes concentrations from the GC-BVOC1 and the PTR-MS, and it is probably related to the underestimation of total monoterpene concentration by the GC technique.

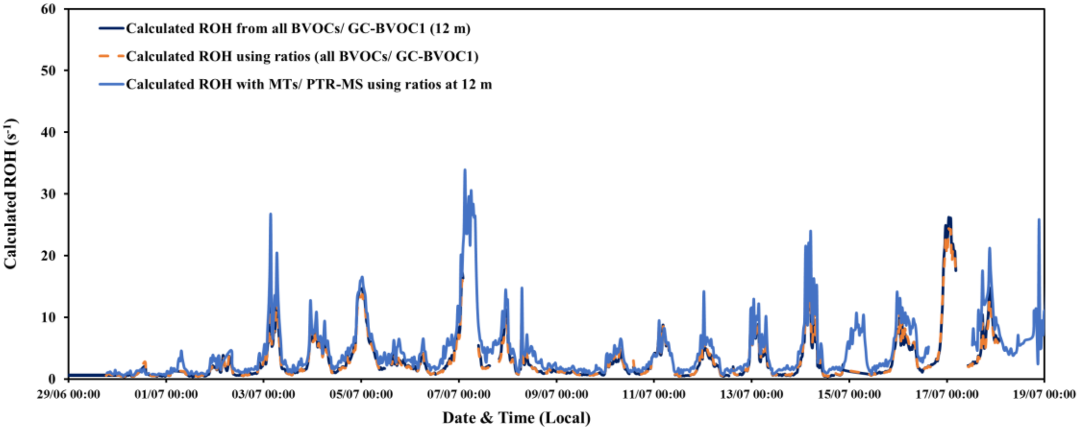

Figure S3(b). OH reactivity calculated for monoterpenes measured with the GC-BVOC1 at 12 m using the concentration and the k rate constant of each monoterpene (dark blue line), with the sum of the concentrations weighted by the ratio of each monoterpene multiplied by the respective rate constant (orange dots), with the sum of monoterpenes measured by the PTR-MS considering the weighted k rate constant reactivity from the monoterpenes measured by the GC-BVOC1 (light blue line).

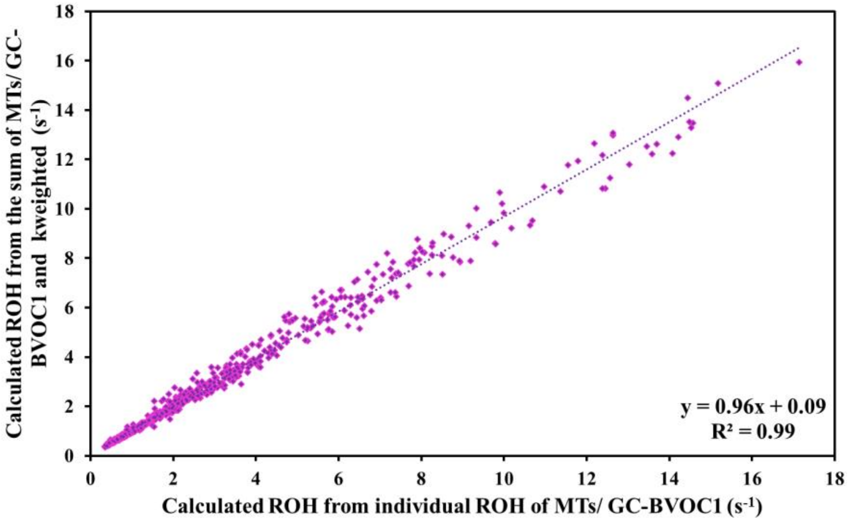

Figure S3(c). Correlation between the calculated OH reactivity from the sum of monoterpenes measured by the GC-BVOC1 multiplied by $k_{weighted}$ with the calculated OH reactivity from individual monoterpenes measured by the GC-BVOC1.

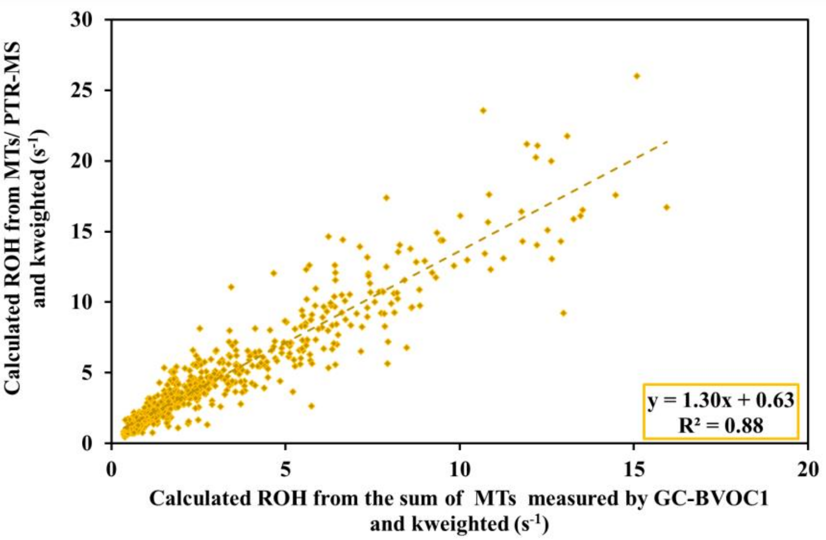

Figure S3(d). Correlation between the calculated OH reactivity from the sum of monoterpenes measured by the PTR-MS multiplied by $k_{weighted}$ and the calculated OH reactivity from the sum of monoterpenes measured by GC-BVOC1 multiplied by $k_{weighted}$.

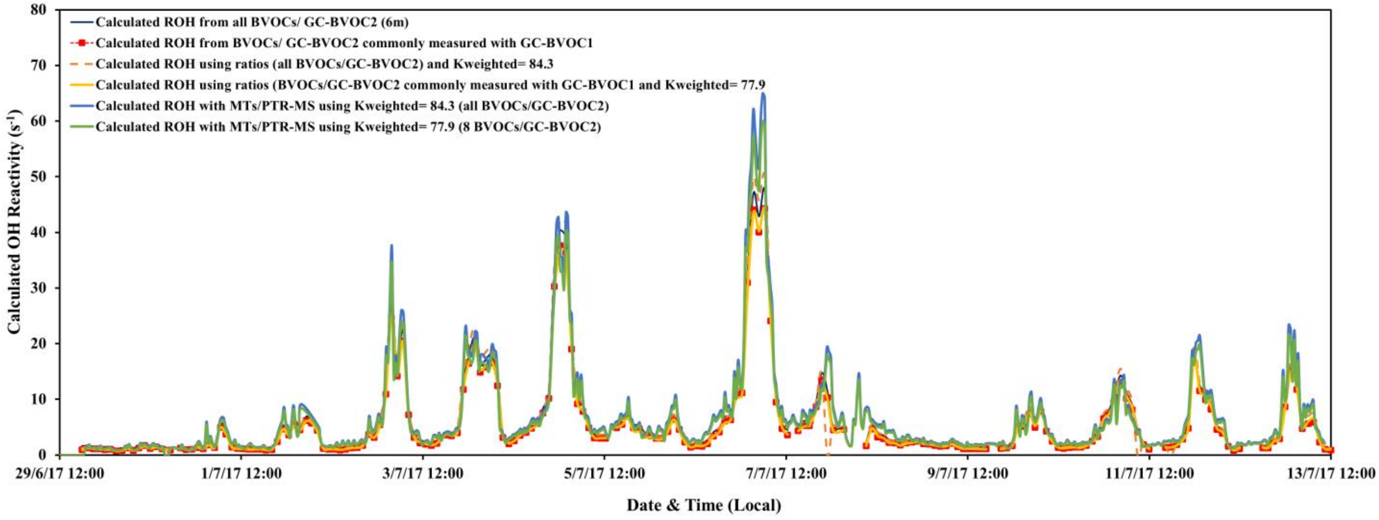

Figure S3(e). OH reactivity calculated from GC-BVOC2 monoterpenes measured at 6 m using the concentration and rate constant of each monoterpene (dark blue line), from GC-BVOC1 monoterpenes commonly measured by the GC-BVOC1 (LSCE) at 12m height (red dashed line), from the total monoterpenes concentration weighted by the ratio of each monoterpene multiplied by the respective rate constant (orange dashed line), from total monoterpenes measured by the PTR-MS considering the weighted reactivity from the monoterpenes measured by the GC-BVOC2 (blue) or the restricted list (corresponding to those commonly measured by the GC-BVOC1 (green)).

Inside canopy (6 m)

The calculated OH reactivity from each monoterpene was also compared at 6 m height, with the one obtained from the ratios for the GC-BVOC2 data and the PTR-MS data (fig. S3e). Ratios calculations were made either by using all the monoterpenes measured by the GC-BVOC2 (14 compounds). In this case the weighted k rate constant was 84.3 x 10^{-12} cm^3 $molecule^{-1}$ s^{-1}. Either based on 8 monoterpenes only, which are the ones commonly measured by the GC-BVOC1. In this case, the weighted k rate constant was 77.9 x 10^{-12} cm^3 $molecule^{-1}$ s^{-1}. As shown in figure S3e, an overall good agreement was seen. However, some overestimations are seen at the peaks when using the data from the PTR-MS data. The calculated OH reactivity at the highest peak is overestimated by approximately 17.5 s^{-1} (36.7%) at the maximum when considering $k_{weighted}$= 84.3 x 10^{-12} cm^3 $molecule^{-1}$ s^{-1} and by 12.5 s^{-1} (26.3 %) when taking $k_{weighted}$= 77.9 x 10^{-12} cm^3 $molecule^{-1}$ s^{-1}.

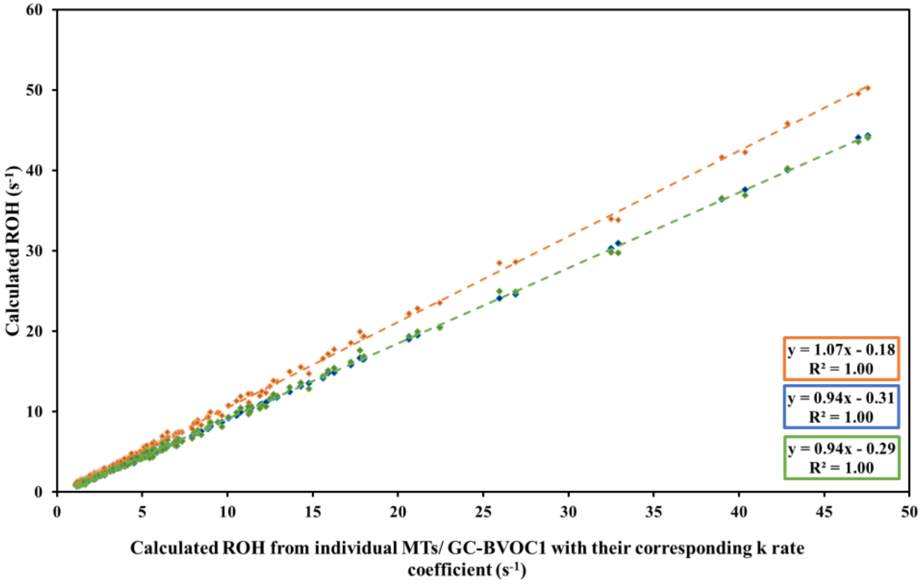

Figure S3(f). Correlation between the calculated OH reactivity from 8 BVOCs measured by GC-BVOC2 (the ones that are commonly measured by GC-BVOC1 (blue)), calculated OH reactivity from the sum of monoterpenes measured by the PTR-MS multiplied by $k_{weighted}$= 84.3 x 10^{-12} cm^3 $molecule^{-1}$ s^{-1} (based on all BVOCs/GC-BVOC2) (orange) and the calculated OH reactivity of the sum of monoterpenes measured by the PTR-MS and multiplied by the weighted k = 77.9 x 10^{-12} cm^3 $molecule^{-1}$ s^{-1} (based on the 8 common BVOCs measured by both GCs) with the calculated OH reactivity from all individual monoterpenes measured by the GC-BVOC1.

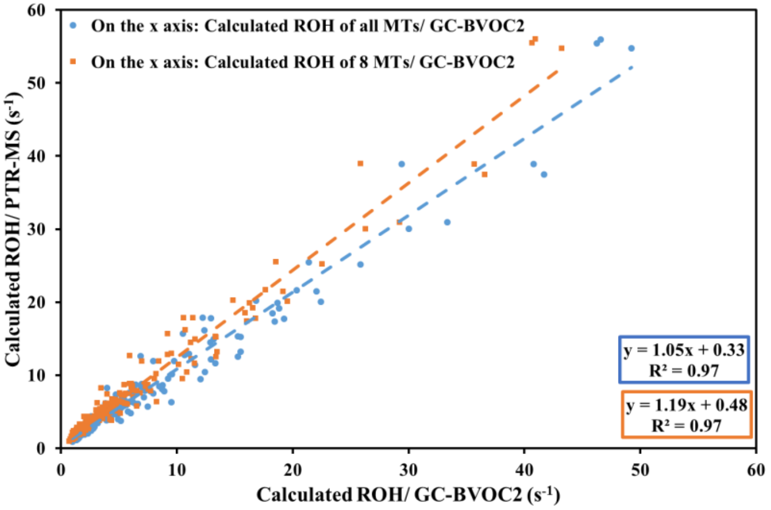

Figure S3(g). Comparison between the calculated OH reactivity from the sum of monoterpenes measured with the PTR-MS and the ones calculated with all the monoterpenes measured by the GC-BVOC2 (blue dots) or with only the monoterpenes commonly measured by the GC-BVOC1 and 2 (orange dots).

Regarding inside canopy measurements, a good agreement (R^2=1, slope of 0.94) exists between the calculated OH reactivity taking each individual monoterpene and the one with the sum of monoterpenes and $k_{weighted}$ (from the mean ratios, k = 77.9 x 10^{-12} cm^3 $molecule^{-1}$ s^{-1}). This agreement was also seen when comparing the sum of monoterpenes measured by the PTR-MS to the sum obtained by GC-BVOC2 (Fig. S2b). It is worth noting that this value of $k_{weighted}$ obtained using GC-BVOC2 compounds commonly measured with the GC-BVOC1 is used for the final calculation of the reactivity and comparisons with measured ones, in order to compare similar data sets at both heights. Finally, when comparing the OH reactivity calculated from the sum of monoterpenes measured by the PTR-MS and $k_{weighted}$ (84.3 x 10-12 cm3 molecule-1 s-1) and the sum of the monoterpenes measured by the GC-BVOC2, a good agreement (Fig. S3g, R^2=0.97, slope of 1.05) was obtained. However, a higher slope was recorded when taking into account only the 8 monoterpenes commonly measured by both GC-BVOC (Fig S3g, slope of 1.19).

Supplementary material 4: Correction of Isoprene concentration measured with the PTR-MS

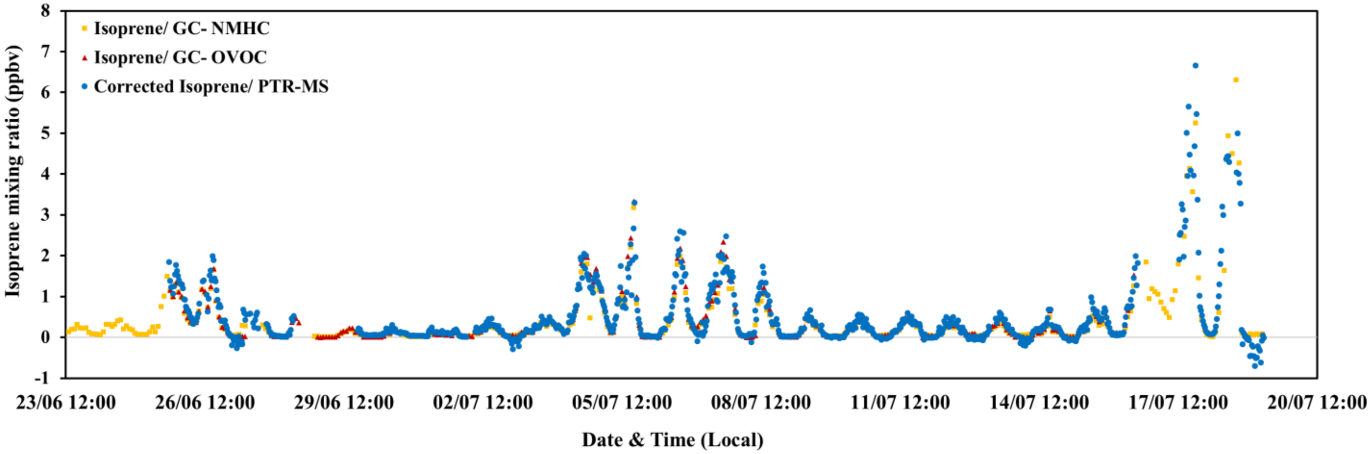

Figure S4(a). Comparison of isoprene concentration measured by three different instruments: corrected data from the PTR-MS (blue points), NMHC (orange points), and OVOC (red points) from 23th of June to 18th of July 2017.

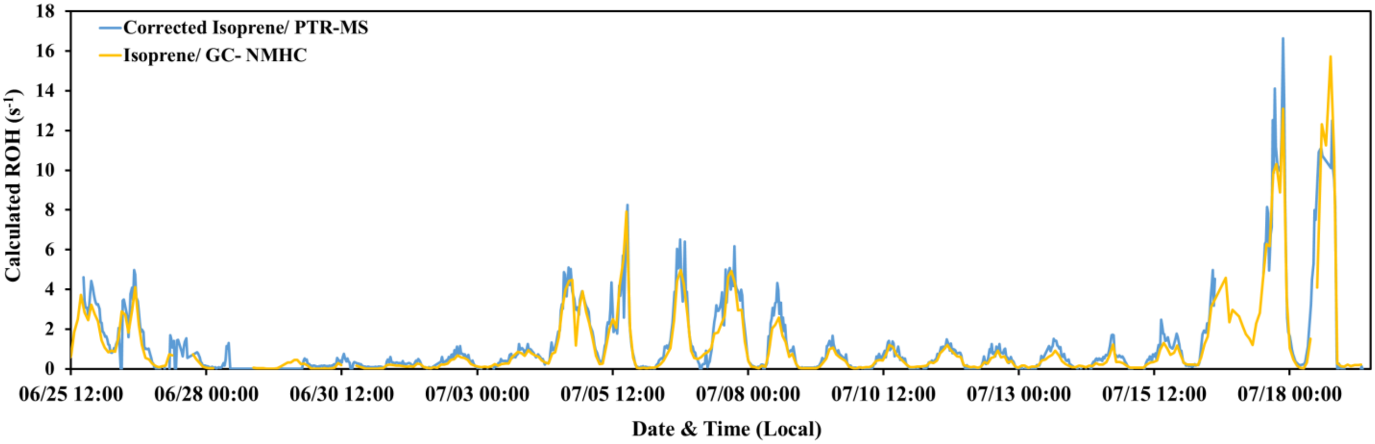

Figure S4(b). Calculated OH reactivity of isoprene measured with the PTR-MS (corrected/ blue) and the GC-NMHC (orange) at 12 m height.

Supplementary material 5: Contribution of OVOCs and NMHCs to OH reactivity above the canopy

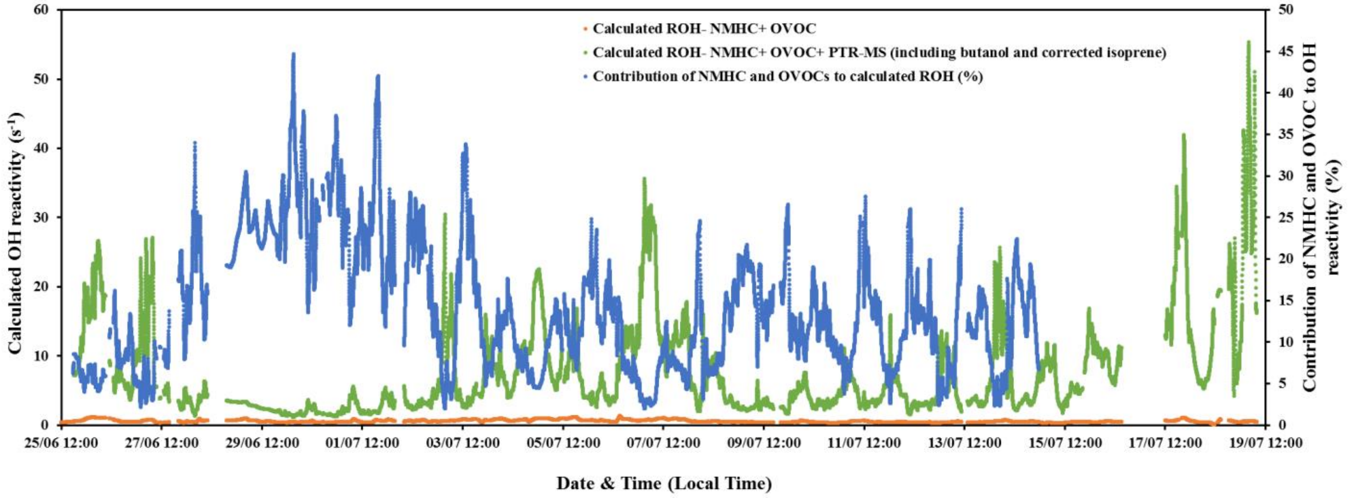

Figure S5. Graph representing the calculated OH reactivity from the GC-NMHC, the GC-OVOC, and the PTR-MS data (including butanol and corrected isoprene) (green dots), from the GC-NMHC and GC-OVOC data alone (orange dots), and the percentage of OH reactivity due to NMHC and OVOC (blue dots).

Supplementary material 6: Butanol (from SMPS exhaust) contribution to OH reactivity

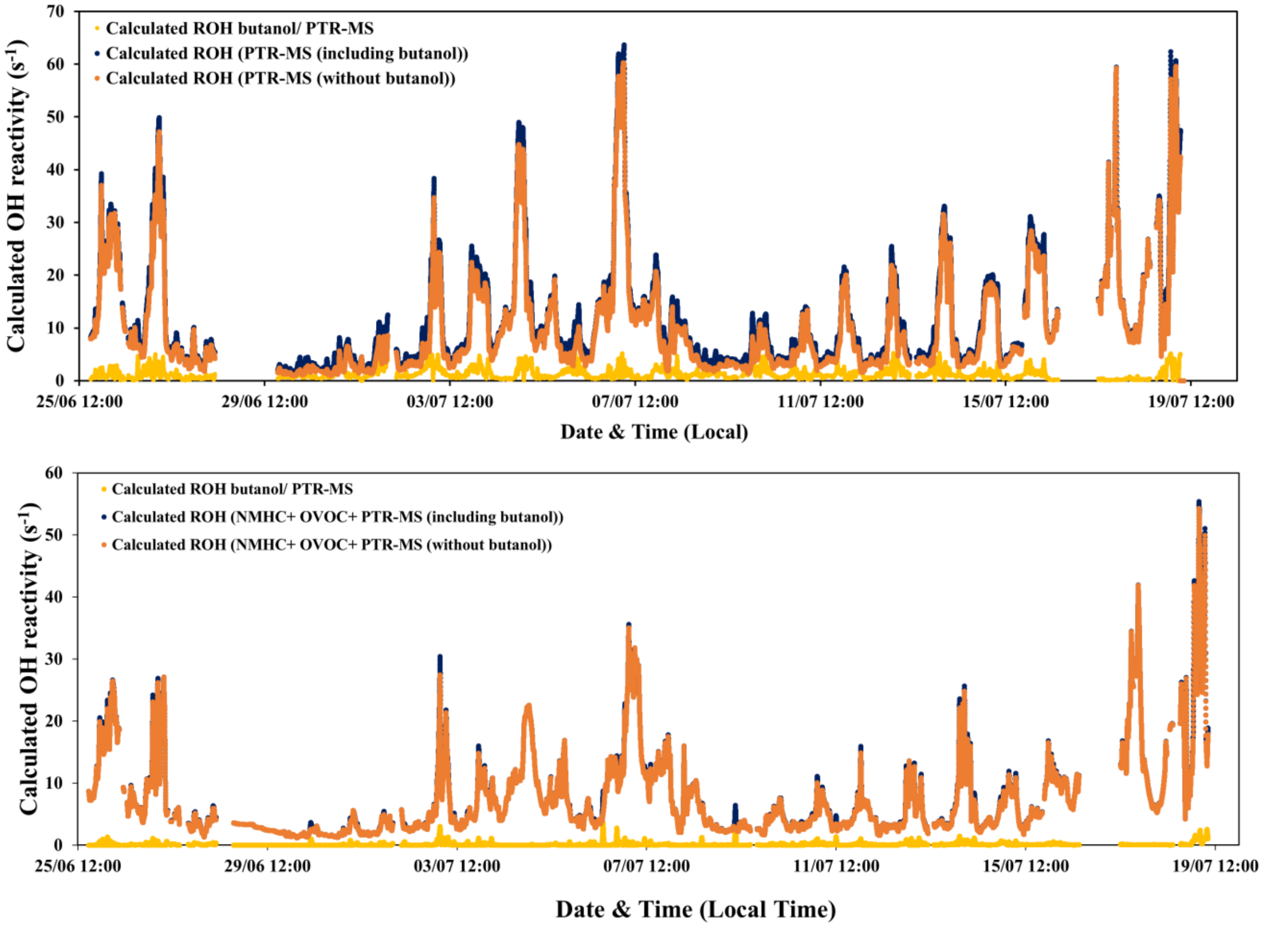

Figure S(6). Butanol contribution to calculated OH reactivity inside (upper graph) and above (lower graph) the canopy.

Supplementary material 7: Assumptions made for OH reactivity calculations

Table S7. Summary of the assumptions taken into account for the calculation of OH reactivity and for the estimation of some compound's contribution to OH reactivity from ancillary measurements.

Problem	Assumption considered
Monoterpenes speciation	Ratios of speciated monoterpenes from GC-BVOC (1 and 2) were taken into account to calculate a weighted k rate constant of the reaction of monoterpenes with OH. The $k_{weighted}$ was used to calculate the reactivity of monoterpenes measured by the PTR-MS.
Measured species only at 12 m	NMHC and OVOC were not taken into account in the calculation of OH reactivity at 12 m and 6 m heights. Their contribution is discussed at 12 m height where they were measured.
Interferences	Isoprene (PTR-MS): A factor of 4 % is considered to correct for the contribution of monoterpenes to the isoprene signal in the PTR-MS. MACR+MVK (*m/z* 71 in PTR-MS): The ratio has been calculated from the GC-OVOC. An average ratio of 0.3 of MACR over the total concentration has been found and used to weight the rate constant for this mass.
Butanol contribution	The contribution of butanol to OH reactivity is estimated at 12 m where it was weak and at 6 m where it was more variable.

Supplementary material 8: Original and resampled data from the LSCE-CRM and UL-FAGE instrument

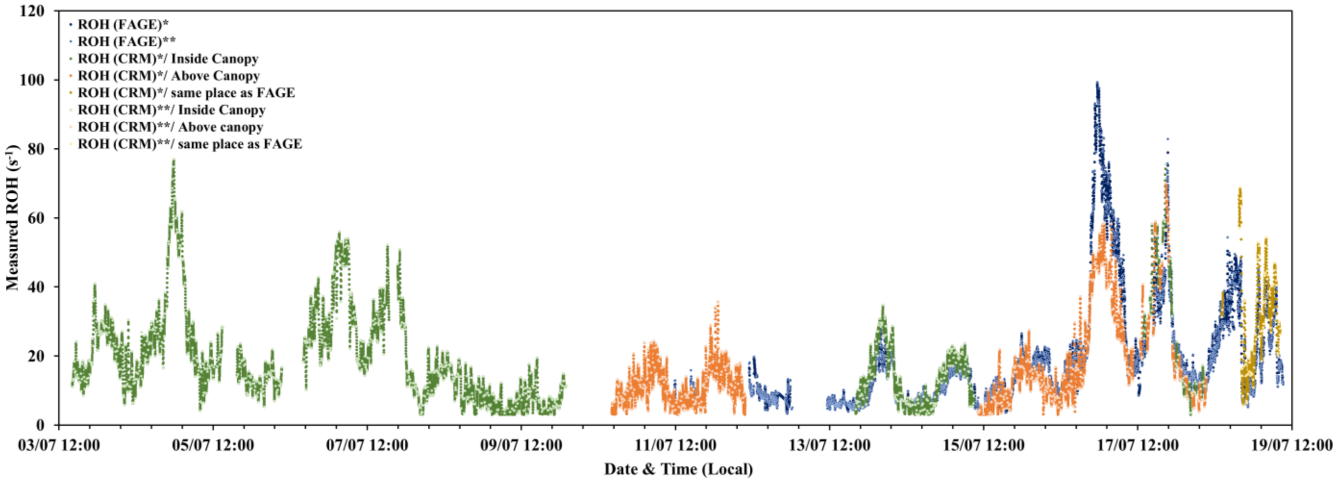

Figure S8. Comparison between the original data set (**) from both OH reactivity instruments and the resampled data set (*).

Supplementary material 9: Summary of day/ night measured, calculated and missing OH reactivity, inside and above the canopy

Table S9. Summary of day/ night averages of measured, calculated and missing OH reactivity, inside and above the canopy. The * indicates above canopy average values when measurements were performed at both heights.

	Day/ Night	**Measured ROH/ LSCE-CRM (s^{-1})**	**Calculated ROH PTR-QiToFMS (s^{-1})**	**Calculated ROH PTR-QiToFMS + other measurements (s^{-1})**	**Missing ROH considering PTR-QiToFMS (s^{-1})**	**Missing ROH considering PTR-QiToFMS + other measurements (s^{-1})**	**Mean Temperature (°C)**	**Mean u* (m s^{-1})**	**Day/ Night state**
Inside Canopy	3rd, July	14.5	5.3	7.8	9.2	6.8	22.9	0.4	Cool
	3rd- 4th, July	25.7	16.1	20.1	9.6	5.6	15.6	0.1	Stable/ Cool
	4th, July	20.0	9.9	12.3	10.0	7.7	26.5	0.6	Warm
	4th- 5th, July	45.6	28.1	32.6	17.5	13.1	21.7	0.2	Stable/ Warm
	5th, July	16.8	8.1	10.8	8.7	6.0	28.1	0.4	Warm
	5th- 6th, July	12.6	4.8	8.5	7.8	4.2	18.9	0.3	Unstable/ Stable/ Warm
	6th, July	22.1	11.0	13.9	11.1	8.2	24.2	0.4	Warm
	6th- 7th, July	37.5	33.6	37.3	3.9	< LOD	20.1	0.1	Stable/ Warm
	7th, July	28.1	18.6	21.6	9.5	6.5	28.3	0.4	Warm
	7th- 8th, July	17.9	9.6	13.1	8.3	4.8	21.2	0.4	Unstable/ Warm
	8th, July	13.2	7.5	10.4	5.7	< LOD	23.0	0.5	Cool
	8th- 9th, July	7.3	2.5	5.3	4.9	<LOD	19.5	0.5	Unstable/Warm
	9th, July	7.4	3.0	5.3	4.4	< LOD	20.9	0.8	Cool
	9th- 10th, July	7.9	3.4	7.1	4.5	< LOD	18.2	0.3	Unstable/ Stable/ Cool
Above Canopy	10th, July	7.7	2.6	4.3	5.1	3.4	20.6	0.5	Cool
	10th- 11th, July	13.0	5.1	6.9	8.0	6.1	17.3	0.1	Stable/ Cool
	11th, July	9.5	3.4	5.2	6.1	4.3	20.9	0.4	Cool
	11th- 12th, July	15.8	6.1	7.9	9.7	7.9	17.0	0.1	Stable/ Cool
	12th, July	10.9	3.0	4.7	7.9	6.2	20.5	0.7	Cool
	12th- 13th, July						18.0	0.1	Stable/ Cool
Inside Canopy	13th, July	6.7	3.1	6.3	3.6	< LOD	20.1	0.4	Cool
	13th- 14th, July	18.7	15.6	19.3	3.1	< LOD	18.0	0.1	Stable/ Cool
	14th, July	8.9	6.7	9.1	< LOD	< LOD	21.2	0.5	Cool
	14th- 15th, July	17.1	13.2	16.3	3.9	< LOD	15.2	0.1	Stable/ Cool
	15th, July a.m	13.3	12.9	15.9	< LOD	< LOD	22.0	0.4	Cool
Above Canopy	15th, July p.m	7.0	4.2	5.9	< LOD	< LOD			
	15th- 16th, July	15.6	10.8	12.7	4.5	< LOD	16.6	0.1	Stable/ Cool
	16th, July	10.0	8.1	9.9	< LOD	< LOD	26.7	0.5	Warm
	16th- 17th, July						21.6	0.1	Stable/ Warm
1h Inside/ 1h Above Canopy	17th, July	41.5/ 35.4*	23.3/ 20.4*	25.1/ 22.4*	18.2/ 15.1*	16.4/ 13.0*	28.9	0.4	Warm
	17th- 18th, July	20.4/ 20.5*	15.3/ 13.4*	17.3/ 15.3*	5.2/ 7.1*	3.1/ 5.2*	23.2	0.3	Unstable/ Warm
	18th, July	11.5/ 8.4*	7.9/ 6.4*	10.1/ 8.1*	3.6/ <LOD	<LOD/ <LOD	30.3	0.5	Warm